

Short communication

Effect of cathode sheet resistance on segmented-in-series SOFC power density

Tammy S. Lai, Scott A. Barnett*

Department of Materials Science and Engineering, Northwestern University, 2220 Campus Dr., Evanston, IL 60201, USA

Received 1 September 2006; received in revised form 24 October 2006; accepted 25 October 2006

Available online 8 December 2006

Abstract

Segmented-in-series solid oxide fuel cells with relatively short cell lengths of 1.4 mm were fabricated with varying LSM cathode current collector thicknesses. Increasing the LSM thickness from 11 to 91 μm yielded a factor of 2–3 area-specific resistance decrease and a similar power density increase. The maximum power density measured at 800 $^{\circ}\text{C}$ was 0.53 W cm^{-2} calculated based on total array area (including interconnect), and 0.9 W cm^{-2} calculated based on active cell area. A segmented-in-series electrical model was used to quantitatively explain the results based on the decreased cathode sheet resistance. The model also showed that the cell lengths were near optimal for maximizing the power density of these cells. © 2006 Published by Elsevier B.V.

Keywords: SOFC; Segmented-in-series; Optimization; Cathode; Modeling

1. Introduction

Recent model calculations [1,2] and experimental results [2] have suggested that segmented-in-series solid oxide fuel cells (SIS-SOFCs) can achieve higher power densities by reducing the cell length L_{cell} below the typical value of $\approx 1 \text{ cm}$ [3–5]. One model predicts an optimal L_{cell} value that minimizes lateral resistance losses across the electrodes while maintaining a large fraction of active cell area (i.e., minimizing interconnect area) [1]. For typical SOFC area-specific resistances of $\approx 0.3 \Omega \text{ cm}^2$ and typical current-collector materials – $\approx 50 \mu\text{m}$ thick (La, Sr)MnO₃ (LSM) and $\approx 20 \mu\text{m}$ thick Ni-yttria stabilized zirconia (YSZ) – highest power densities were predicted for $L_{\text{cell}} = 1\text{--}2 \text{ mm}$. Furthermore, decreasing the cathode-side sheet resistance was predicted to allow increased power density; note that the main resistance loss is on the cathode side due to the substantially higher resistivity of LSM compared to Ni-YSZ. Power densities approaching 1 W cm^{-2} were predicted, compared to experimental SIS-SOFC power densities of only $\approx 0.1\text{--}0.3 \text{ W cm}^{-2}$ [2,4,5].

In this letter, we studied the performance of SIS-SOFCs with $L_{\text{cell}} = 1.4 \text{ mm}$ for varying LSM cathode current collector thick-

nesses. One aim of this study was to compare the model results described above with experimental SIS-SOFCs. Specifically, the present work was done to check the model prediction that power density should increase with increasing LSM thickness (decreasing cathode sheet resistance), and then saturate for large-enough thickness. Another aim was to investigate whether optimized L_{cell} and cathode sheet resistance could lead to higher power densities than previously reported.

2. Experimental procedure

The fabrication procedure of the four-cell SIS-SOFC arrays was similar to that described previously [2]. The cell supports were porous partially stabilized zirconia (PSZ) pellets formed by pressing (19 mm diameter, 0.5 mm thick post-firing). After bisque firing at 1250 $^{\circ}\text{C}$, the Ni-YSZ anode, YSZ electrolyte, and Pt-YSZ interconnect (45 vol.% Pt) were applied by screen printing. The support and active layers were then fired at 1400 $^{\circ}\text{C}$ for 4 h. Subsequently, a LSM cathode active layer, containing 50 vol.% YSZ, was printed and fired at 1175 $^{\circ}\text{C}$. The LSM-YSZ layer was followed by 1–4 prints of pure LSM current collector. In order to avoid cracking of overly thick cathode layers, the cathodes were fired at 1125 $^{\circ}\text{C}$ for up to two LSM layers, with an additional firing at 1125 $^{\circ}\text{C}$ for samples with three or four layers. All cathode firing steps were 1 h in duration. The

* Corresponding author. Tel.: +1 847 491 2447; fax: +1 847 491 7820.
E-mail address: s-barnett@northwestern.edu (S.A. Barnett).

LSM layers were assessed using cross-sectional scanning electron microscopy, checking the four cells in each array to obtain a truly representative thickness value. The cells were all made in the same batch and kept as identical as possible, except for the varied cathode thickness.

A four-point geometry was used to measure the conductivity of the same screen printed and fired LSM cathodes ($2\text{ mm} \times 9\text{ mm}$) on PSZ supports as used in the SIS-SOFCs. Gold paste was used to paint linear contacts onto the bars, and to attach silver wire leads. The measured sheet resistances ranged from $24\ \Omega\ \square^{-1}$ for the thinnest LSM layer ($11\ \mu\text{m}$) to $2.9\ \Omega\ \square^{-1}$ for the thickest LSM layer ($91\ \mu\text{m}$). Measured conductivities were $37\text{--}38\ \text{S cm}^{-1}$, irrespective of LSM thickness and temperature (from 600 to $800\ ^\circ\text{C}$), in reasonable agreement with reported values for LSM with similar porosity [6]. The $\approx 20\ \mu\text{m}$ thick LSM–YSZ cathode layer had a low conductivity relative to pure LSM and, hence, had a minor contribution to the overall sheet resistance.

SOFC current–voltage data were collected from the segmented-in-series arrays using a setup similar to that typically used for single SOFC testing [7]. The samples were sealed to alumina or quartz tubes using silver paste (Shanghai Research Institute of Synthetic Resins, DAD-87). Gold and silver pastes were used to attach silver wire contacts to the end electrodes. Humidified hydrogen ($3\% \text{H}_2\text{O}$) was flowed through the tube into the support/anode side of the SIS-SOFC, generally at a rate of $100\ \text{sccm}$, while the cathode side was exposed to stagnant air. Power densities and area-specific resistances were typically calculated based on the total area of the four-cell array. Power density values normalized to active cell area are also given in some cases where noted, and were a factor of 1.7 higher because the active cell area was 58% of the total array area.

3. Results and discussion

Fig. 1 shows the voltage and power density versus current density for arrays with 11 and $91\ \mu\text{m}$ thick LSM layers, measured at $600\text{--}800\ ^\circ\text{C}$. The arrays yielded similar open circuit voltages of $0.90\text{--}0.98\ \text{V}$. These values are higher than in a prior report [2], apparently due to reduced gas leakage based on a higher density in the present Pt-YSZ interconnects. The current density and maximum power density increased with increasing temperature, typical of SOFCs. The maximum power densities were substantially higher for the thicker LSM current collector, e.g., $0.53\ \text{W cm}^{-2}$ ($0.9\ \text{W cm}^{-2}$ based on cell active area) versus $0.19\ \text{W cm}^{-2}$ ($0.28\ \text{W cm}^{-2}$ based on cell active area) at $800\ ^\circ\text{C}$. The voltage versus current density curves showed a general concave-up curvature; the exception was for the array with thicker LSM, where there was evidence of a limiting current at relatively high current densities $>1.8\ \text{A cm}^{-2}$ ($3\ \text{A cm}^{-2}$ based on cell active area). The current–voltage curves were generally closer to linear at the lesser cathode thickness, perhaps reflecting a larger component of lateral cathode ohmic resistance loss.

Fig. 2 shows the array area-specific conductance (and resistance), estimated from the low-current slopes of the current–voltage curves (filled symbols), versus LSM thickness (and sheet resistance). The area-specific conductance generally

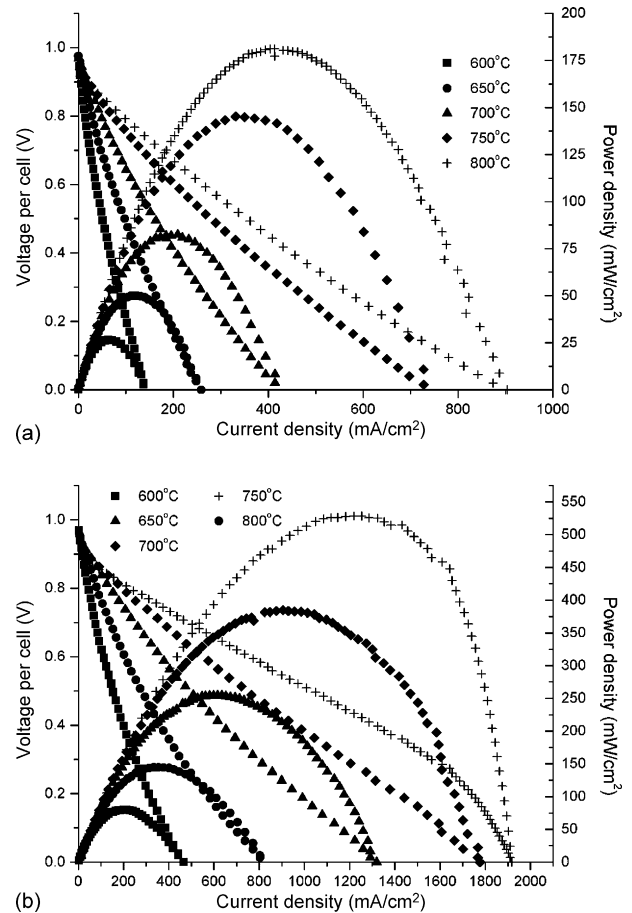


Fig. 1. Voltage per cell and power density vs. current density for cells with $11\text{-}\mu\text{m}$ -thick LSM layers (a) and $90\text{-}\mu\text{m}$ -thick LSM layers. (b) Power density and current density were calculated based on total array area.

increased with increasing cathode thickness, although there was considerable scatter in the data.

Predictions based on the segmented-in-series model in Ref. [1] were compared with the above experimental results. The calculation included the cell resistance R_{cell} (i.e., electrolyte

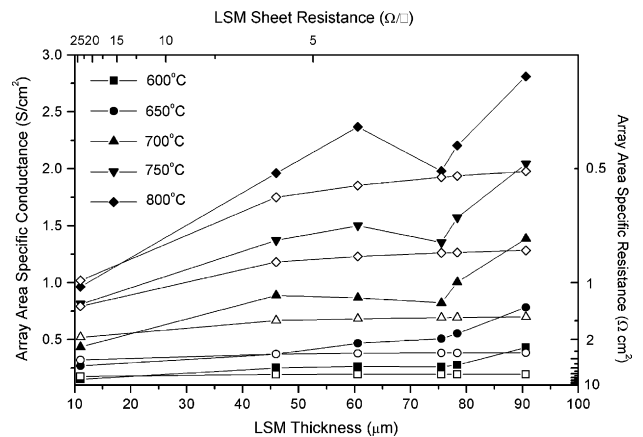


Fig. 2. Array area-specific conductance and resistance values versus LSM current-collector thicknesses, at various temperatures. Filled symbols indicate values measured from the low-current slope of the experimental current–voltage data. Open symbols show the dependence calculated using the model.

resistance, anode and cathode polarization resistance), resistances associated with lateral current transport across the anode and cathode, and the interconnector resistance. The latter term was negligible in the present case due to the high conductivity of the Pt-YSZ interconnector. R_{cell} values were chosen at each temperature and assumed to be the same for all cells irrespective of the LSM thickness. That is, the LSM current collector thickness was assumed to have negligible impact on the cathode polarization resistance; this is reasonable because the LSM–YSZ cathode thickness of $\approx 20 \mu\text{m}$ was greater than the thickness normally thought to contribute to electrochemical reactions [8]. Also, any additional concentration polarization due to the LSM was likely negligible [9]. The key parameters used in the resistance-loss calculation are the 1.4 mm cell length and the current-collector sheet resistance. The 0.45–0.5 mm wide current-collector segment, that connects each cell to the adjacent interconnector, was included in the resistance loss.

The predicted area-specific conductance values are compared with the experimental data in Fig. 2. The predicted array conductance (open symbols) increased with increasing cathode thickness, but saturated for thicknesses $>75 \mu\text{m}$. The overall agreement with the experimental data is reasonably good, despite the scatter in the experimental data. Note that the predicted variation at lower temperatures is quite small—this is the result of the relatively large R_{cell} value, which tends to overshadow the cathode resistance contribution for these short-length cells. The R_{cell} values used in the calculations are plotted in Fig. 3. Note that they followed the expected Arrhenius dependence on temperature, with an activation energy of $\approx 1.1 \text{ eV}$. This value is reasonable assuming that it is a combination of the ohmic resistance of the YSZ electrolyte (activation energy $\approx 1.0 \text{ eV}$ [10]) and the electrode polarization resistance (e.g., $\approx 1.5 \text{ eV}$ for LSM–YSZ cathodes [8]).

The deviation of the experimental results from the model may be explained by sample-to-sample variations in our experiments. The array with the largest cathode thickness was the only case that showed a very large deviation, with a much higher power density than predicted. There may have also been a systematic variation. That is, an additional firing step was used in cathodes

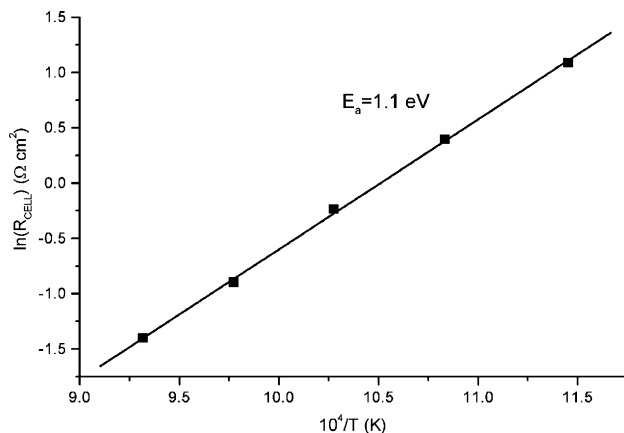


Fig. 3. R_{CELL} values used to obtain the calculated curves shown in Fig. 2, plotted vs. inverse temperature. The line shown is a fit assuming Arrhenius behavior with an activation energy of 1.1 eV.

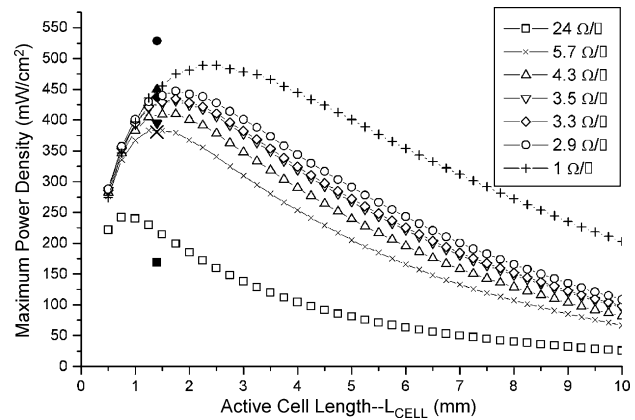


Fig. 4. Calculated maximum power densities at 800°C vs. active cell length for SIS-SOFCs with various cathode sheet resistances (open symbols), taking $R_{\text{CELL}} = 0.25 \text{ cm}^2$. The maximum power density values experimentally measured at 800°C with $L_{\text{CELL}} = 1.4 \text{ mm}$ are also shown for comparison (solid symbols).

with three or four LSM prints ($\geq 60 \mu\text{m}$ thickness), resulting in additional sintering of the electrochemically active LSM–YSZ cathode layer that might have modified the microstructure and yielded improved electrochemical performance. However, our prior work on these cathodes did not show a substantial change in polarization resistance with LSM–YSZ firing time.

Fig. 4 shows the predicted maximum power density at 800°C versus L_{cell} , compared with the experimental data at $L_{\text{cell}} = 1.4 \text{ mm}$. This was calculated for a total inactive length (interconnector plus electrode gaps) of 1.0 mm. This plot illustrates that these arrays had L_{cell} values near the optimal for the present operating conditions, and again shows the relatively good agreement with the model (except for the largest cathode thickness). According to the calculation, lowering the cathode sheet resistance decreased the cathode resistance loss, shifting the optimal L_{cell} from 0.8 to 2.5 mm and increasing the maximum power density from 240 to 480 mW cm^{-2} . A similar dependence was predicted at each temperature but the optimal L_{cell} values were larger at lower temperatures, e.g., at 600°C the optimal L_{cell} increased to the range 2.5–4.75 mm with increasing cathode thickness. This was explained by the larger R_{cell} values at lower temperature, such that cathode resistance losses only became important for larger cell lengths. Of course, predicted and measured power densities were quite low at 600°C .

4. Conclusions

For the present cell length of 1.4 mm, LSM thicknesses $>75 \mu\text{m}$ are sufficient to minimize current collection losses. It may be desirable in future SIS-SOFC designs to increase L_{cell} , e.g., to $\sim 2.5 \text{ mm}$; Fig. 4 illustrates that this can yield higher power density if lower sheet resistance cathodes are utilized. In particular, one of the curves in Fig. 4 was calculated for a low sheet resistance of $1 \Omega \square^{-1}$ (corresponding to a thicker, $\approx 260 \mu\text{m}$, LSM layer) and shows a 10% higher maximum power density than the thinner LSM layers. However, it would likely be impractical to do the large number of screen prints required to make such thick LSM layers. A fabrication technique that could

produce thick patterned cathode layers onto segmented-in-series cells would be useful. Alternatively, a more conductive current collector material could be used to achieve the same effect; for example, Ag-based current collectors have been used to achieve low resistance losses and good power density (0.3 W cm^{-2} at 725°C) for cell lengths of 8 mm [11].

The highest measured power density accounting for the full SIS-SOFC area was $\approx 0.53 \text{ W cm}^{-2}$ at 800°C . This corresponds to $\approx 0.9 \text{ W cm}^{-2}$ calculated using only the active cell area. There was a recent report of a power density of $\approx 0.35 \text{ W cm}^{-2}$ at 0.58 V at 835°C for SIS-SOFCs with a similar materials set and a cell length of 10 mm [5,12]. However, it was not clarified whether this was calculated using active or full cell area, nor were layer thicknesses given. In any case, the present power densities were substantially higher, despite the lower temperature of 800°C , presumably due to the shorter cell lengths.

Acknowledgements

The authors gratefully acknowledge the assistance of Manoj Pillai, Yi Jiang, Negar Mansourian, and Ilwon Kim of Functional Coating Technology, who provided valuable information about the fabrication of the PSZ supports, and for providing the Pt-YSZ interconnect inks used in this study. We also gratefully

acknowledge financial support from the Department of Energy Solid State Energy Conversion Alliance.

References

- [1] T.S. Lai, S.A. Barnett, *J. Power Sources* 147 (2005) 85–94.
- [2] T.S. Lai, J. Liu, S.A. Barnett, *Electrochem. Solid-State Lett.* 7 (2004) A78–A81.
- [3] A.O. Isenberg, *Solid State Ionics* 3/4 (1981) 431–437.
- [4] J. Iritani, K. Kugami, N. Komiyama, K. Nagata, K. Ikeda, K. Tomida, in: SOFC., V.I.L., H. Yokokawa, S.C. Singhal (Eds.), 2001–16, The Electrochemical Society Proceedings Series, Tsukuba, Ibaraki, Japan, 2001, p. 63.
- [5] F.J. Gardner, M.J. Day, N.P. Brandon, M.N. Pashley, M. Cassidy, *J. Power Sources* 86 (2000) 122–129.
- [6] J. Holc, D. Kuscer, M. Hrovat, S. Bernik, D. Kolar, *Solid State Ionics* 95 (1997) 259–268.
- [7] Z. Zhan, S.A. Barnett, *Science* 308 (2005) 844.
- [8] E.P. Murray, T. Tsai, S.A. Barnett, *Solid State Ionics* 110 (1998) 235–243.
- [9] F. Zhao, A.V. Virkar, *J. Power Sources* 141 (2005) 79–95.
- [10] N.Q. Minh, *J. Am. Ceram. Soc.* 76 (1993) 563–588.
- [11] D.J. St. Julien, T.D. Ketcham, M.E. Badding, J.L. Brown, P. Diep, K.A. Wexell, R.R. Wusirika, J.E. Cortright, J. Olenick, *Fuel Cell Seminar Abstracts*, 2005, p. 73.
- [12] P. Costamagna, A. Selimovic, M. Del Borghi, G. Agnew, *Chem. Eng. J.* 102 (2004) 61–69.